

AC CONDUCTIVITY STUDIES OF P-TOLUENESULFONIC ACID DOPED POLYANILINE-SODIUM ALGINATE COMPOSITES

Y. T. RAVIKIRAN, S. KOTRESH, S. C. VIJAYA KUMARI,^{*} K. C. SAJJAN,^{**}
 B. S. KHENED^{***} and S. THOMAS^{****}

^{}Department of PG Studies in Physics, Government Science College, Chitradurga-577 501, India*

^{}Department of Physics, SJM College of Arts, Science and Commerce, Chitradurga-577 501, India*

*^{**}Department of Physics, Veerasaiva College, Bellary-583104, India*

*^{***}Department of Electrical and Electronics Engineering BITM, Bellary-583104, India*

*^{****}Centre for Nanoscience and Nanotechnology, Mahatma Gandhi University,*

Kottayam-686 560, India

✉ Corresponding author: Y. T. Ravikiran, ytrcta@gmail.com

In this work, an attempt has been made to enhance Alternating Conduction (AC) properties of sodium alginate/polyaniline (SA/PANI) composites. So, four SA/PANI composites with different concentrations of PANI have been synthesized at room temperature using the chemical polymerization technique. The interaction of PANI with SA during the formation of the composite was examined by Fourier transform infrared spectroscopy (FTIR) analysis. The arrangement of PANI chains in the composites and their crystallinity were investigated by X-ray diffraction studies. The submicron size and the morphology of the composites were confirmed by the scanning electron microscopy technique. Increased AC conductivity of the composites at room temperature in the frequency range 100 Hz to 1 MHz was confirmed. Of the four composites, the complex plane impedance plot of SA/PANI-60% composite was simulated to find an equivalent resistance-capacitance circuit. Based on these predictions, the SA/PANI-60% composite has been tested and it proved to be a good material capable of sensing humidity at room temperature.

Keywords: polyaniline, sodium alginate, polymer composites, electrical properties, humidity sensor

INTRODUCTION

The interaction of biopolymers with conducting polymers may generate interesting biopolymer/conducting polymer composites, which find applications where electrical conductivity is desirable, such as in artificial nerves, sensors and actuators.¹ The blending of naturally available biopolymers such as rubber, wax etc. with conducting polymers such as polyaniline and polypyrrole has been shown to alter the physical and electrical properties of both polymers.² So, in the present research, with the intention of increasing the scope and versatility of biopolymer/conducting polymer composites, SA/PANI composites have been synthesized and studied to enhance their AC electrical conductivity and humidity sensing properties.

SA is a biopolymer of sodium salt of alginic acid and is a naturally occurring nontoxic polysaccharide found in brown algae.³ It is an insulator containing two uronic acids, α -L-guluronic acid and β -D-mannuronic acid and its chemical structure is shown in Fig. 1(a). Further,

SA is a hydrophobic polymer and shows remarkable gelatin properties in the presence of divalent ions and hence it has been extensively studied for various specific biomedical applications *viz.*, as a drug carrier, as a haemostatic material and as a material for fuel cell.⁴⁻⁶

Recent studies on PANI throw light on its structure (Fig. 1(b)), which offers unique characteristics like controllable chemical and electrical properties, simple preparation, low cost and excellent environmental stability, due to which they find a wide variety of applications, such as in the development of super capacitors, rechargeable batteries and sensors.⁷⁻¹⁰

Thus, these properties of SA and PANI have encouraged us to exploit the properties of SA/PANI composites to enhance their AC electrical conductivity at room temperature. In particular, PANI when combined with SA is expected to increase its humidity sensing property

at room temperature without compromising its good sensing characteristics.

In the present work, four composites of *p*-toluenesulfonic acid (PTSA) doped PANI have been synthesized by polymerizing aniline in the presence of SA by varying aniline concentration in aqueous medium. These composites were then

characterized using FTIR, XRD and SEM techniques. Further, the AC electrical response properties of the composites at room temperature in the frequency range 100 Hz to 1 MHz were studied. The results of the studies were applied to the SA/PANI-60% composite to examine its performance as a resistive type humidity sensor.

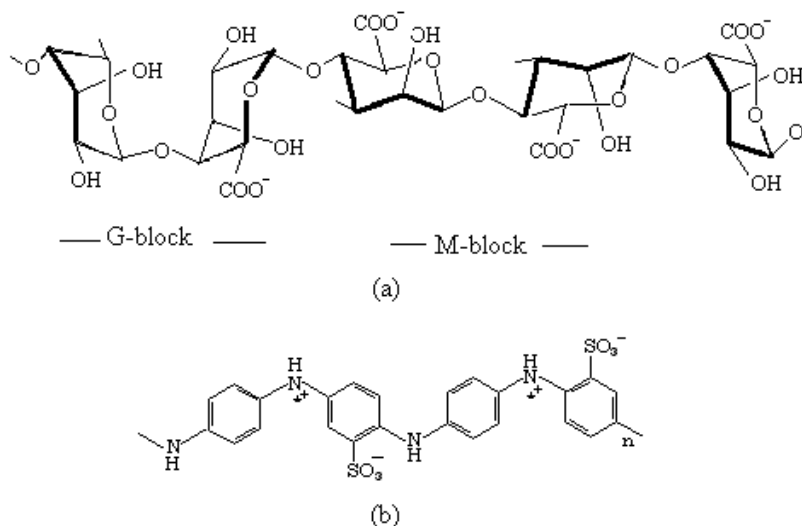


Figure 1: Chemical structure of (a) SA, (b) PTSO doped PANI

EXPERIMENTAL

All chemicals used were reagents of analytical grade and were purchased from s.d. Fine Chemicals, Mumbai, India. For synthesizing SA/PANI composites, initially, 1 g of SA was dissolved in 80 mL of water and stirred for 8-10 hours using a magnetic stirrer. A mixture of *p*-toluenesulfonic acid (PTSA) and aniline (in the ratio 1:5) dissolved in 10 mL of water was added to the above mixture and was again stirred well. Then, a previously prepared solution of ammonium peroxydisulfate (APS) in 10 mL of water (maintaining aniline:APS = 1:1.2) was added to the above mixture to initiate polymerization of aniline. The reaction was allowed to proceed for 4 hours. The composite was isolated by centrifugation of the reaction mixture and then washed repeatedly with distilled water and acetone to remove impurities. The yield of the composite so obtained was found to vary from 1.5 g to 2.5 g. The amount of aniline in the reaction mixture was 0.2, 0.4, 0.6 and 0.8 mL to obtain respectively 20, 40, 60 and 80 wt% of PANI in the SA/PANI composites.

The FTIR spectra of the SA and SA/PANI composites were recorded over a wavenumber range of 400 to 4000 cm⁻¹, using a JASCO 480 Plus FT-IR spectrometer. X-ray diffraction spectra of the SA and

SA/PANI composites were recorded by a Siemens/D-5000 X-ray diffractometer using CuK α radiation ($\lambda = 1.5406 \text{ \AA}$). The scanning electron micrographs of the SA and SA/PANI composites were obtained using a Hitachi S-520 scanning electron microscope to analyze their morphology and microstructure.

AC response parameters of the SA/PANI composites in the form cylindrical pellets were measured at room temperature using a Hioki Model 3532-50 programmable LCR meter (Japan) over the frequency range of 100 Hz to 1 MHz. The humidity sensing response of the SA/PANI-60% composite was studied on samples in the form of thin films coated on a glass plate using a spin coating unit (Delta Scientific Pvt. Ltd, India, Model Delta Spin I). The film was placed in a special glass chamber, where humidity could be controlled by saturated salt solutions and monitored using a humidity meter (Mextech-DT-615). Room temperature sensing response studies of the composite to humidity was carried out using the same LCR meter at a frequency of 100 Hz.

RESULTS AND DISCUSSION

FTIR spectral analysis

The FTIR spectra of the SA and SA/PANI composites (SA/PANI-40%, SA/PANI-60%) are

given in Fig. 2. The IR spectrum of SA shows absorption bands at 1629 cm^{-1} and 1422 cm^{-1} corresponding to COO^- asymmetric stretching and COO^- symmetric stretching of carboxylate salt groups, respectively. Further, bands around 1304 cm^{-1}

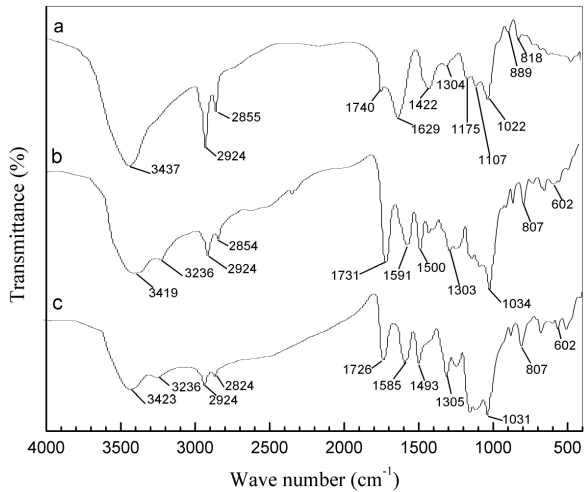


Figure 2: Fourier transform infrared spectra of (a) SA, (b) SA/PANI-40% and (c) SA/PANI-60%

The FTIR spectra of SA/PANI-40% and SA/PANI-60% composites show characteristic absorption bands around 3423 cm^{-1} (N-H stretching), 3236 cm^{-1} (C-H stretching), 1591 cm^{-1} (C-N stretching of quinoid rings of PANI), 1500 cm^{-1} (C-N stretching of benzene rings of PANI), 1303 cm^{-1} (aromatic C-N stretching indicating the presence of a secondary aromatic amine group), 1034 cm^{-1} (due to the SO_3^- group of PTSA), 807 cm^{-1} (due to para-disubstituted aromatic rings indicating conducting PANI formation) and 602 cm^{-1} (C-H out of plane bending vibration).⁷ The observed prominent bands of SA and PANI in the spectra of the composites suggest good interaction between PANI and SA. However, one can notice the shifts in the absorption bands of PANI in the composites, which could be an indication of the changes in the physical properties of SA, as well as in those of pure PANI.

X-ray diffraction studies

X-ray diffraction patterns of SA and SA/PANI composites (SA/PANI-40%, SA/PANI-60%) are

cm^{-1} (C-O stretching), 1175 cm^{-1} (C-C stretching), 1107 cm^{-1} (C-O stretching), 1022 cm^{-1} (C-O-C stretching) and 889 cm^{-1} (C-O stretching) are attributed to the saccharide structure of SA.⁶

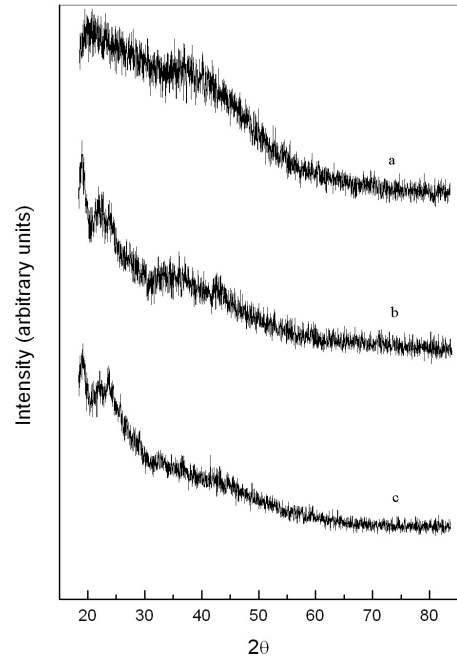


Figure 3: X-ray diffraction spectra of (a) SA, (b) SA/PANI-40% and (c) SA/PANI-60%

shown in Fig. 3. The XRD spectrum of SA shows a broad hump at $2\theta = 38^\circ$, which indicates its amorphous nature.⁶ The XRD pattern of the composite shows two peaks at $2\theta = 20^\circ$ and $2\theta = 24^\circ$ corresponding to PANI, which may be attributed to the periodicity parallel and perpendicular to the polymer chains.¹¹ Further, one can observe that the broadness of the hump corresponding to SA in the composites decreases with increasing wt% of PANI, indicating a more ordered structure.

Scanning electron microscopy

The SEM of pure SA and of the composites (SA/PANI-40%, SA/PANI-60%) are shown in Fig. 4. It can be seen that pure SA exhibits a bulky and rigid backbone structure, whereas SA/PANI composites show submicron particles, along with combinations of a few particles into larger grains of irregular shape. It is well known that PANI has a flexible backbone, which favours closer molecular packing and crystallization when combined with SA. Therefore, the crystallinity of

the composites might have increased with the addition of aniline in the composites.

AC conductivity studies

The variation of the real part of complex AC conductivity $\sigma'(f)$ for SA/PANI composites versus frequency is f given in Fig. 5. It has been found that $\sigma'(f)$ remains almost constant over the low frequency range, *i.e.* from 100 Hz to critical frequency f_c , and then increases above f_c . This is

attributed to the hopping mechanism of the charge carrier.¹³ In the low frequency region, the conductivity of the composites lies in the range 10^{-7} - 10^{-4} S/cm⁻¹. The dependence of $\sigma'(f)$ (at 10 kHz) on PANI content in the composite is given in Fig. 6. It is seen that $\sigma'(f)$ increases with increasing wt% of PANI, which indicates an increase in the crystallinity of the composite, as supported by XRD and SEM studies.

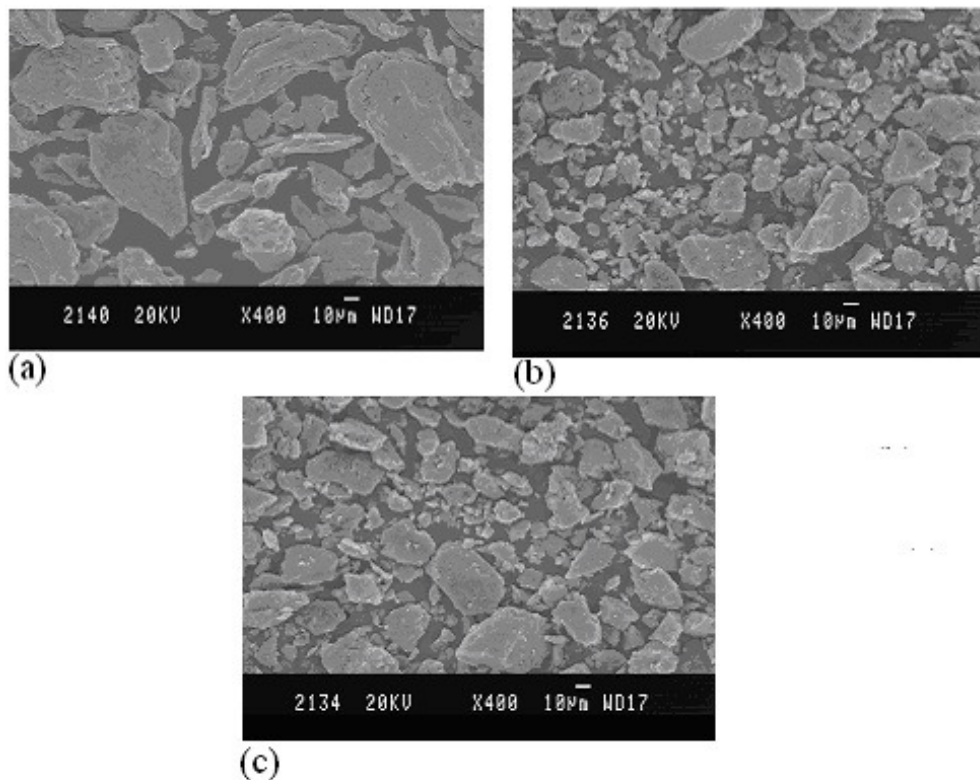


Figure 4: Scanning electron micrographs of (a) SA, (b) SA/PANI-40% and (c) SA/PANI-60%

To examine the validity of the power law, the graph of $\log \sigma'(f)$ vs $\log f$ has been plotted. For each composite, a straight line was obtained with a slope equal to the exponent s . The straight lines fitted to the experimental data by the method of least-squares for frequencies above f_c (shown in Fig. 7) indicate that for frequencies above f_c , $\sigma'(f)$ obeys the power law for each of the composites with a power law index S . The best fitted values of S are given in Table 1. It was found that S lies between 0.2 ± 0.01 and 0.6 ± 0.01 , confirming that conductivity is due to hopping of charge carriers.¹²

For further understanding the AC response of the SA/PANI composites, the f_c obtained from the

typical plot for SA/PANI-60% composite is shown in Fig. 8. The intercept of the plot of $\log \sigma'(f)$ vs $\log \sigma''(f)$ shows a linear dependence for the imaginary part of AC conductivity ($\sigma''(f)$), whereas $\sigma'(f)$ shows a non-linear trend. The same results were obtained for various wt% of PANI in the composites and are shown in Fig. 9. It was found that f_c increased with increasing wt% of PANI. This result was expected, since f_c is known to increase with conductivity.¹³ The entire AC electrical response of the composites as measured through different parameters is summarily shown in Table 1, which also helps to know the interdependence of these parameters.

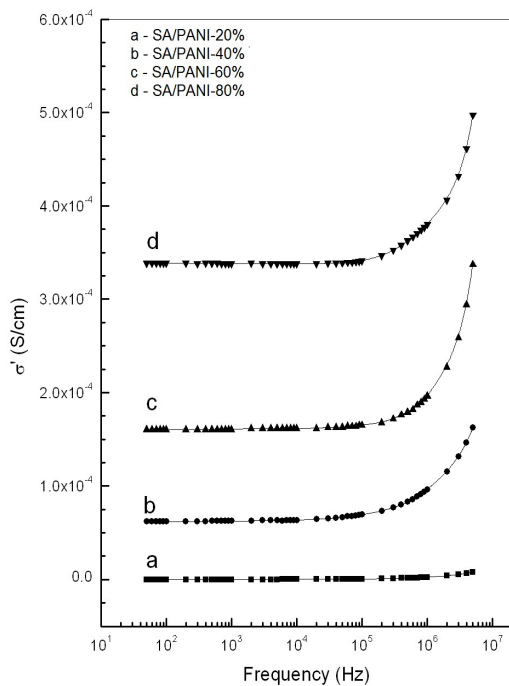


Figure 5: Frequency dependence of AC conductivity of SA/PANI composites

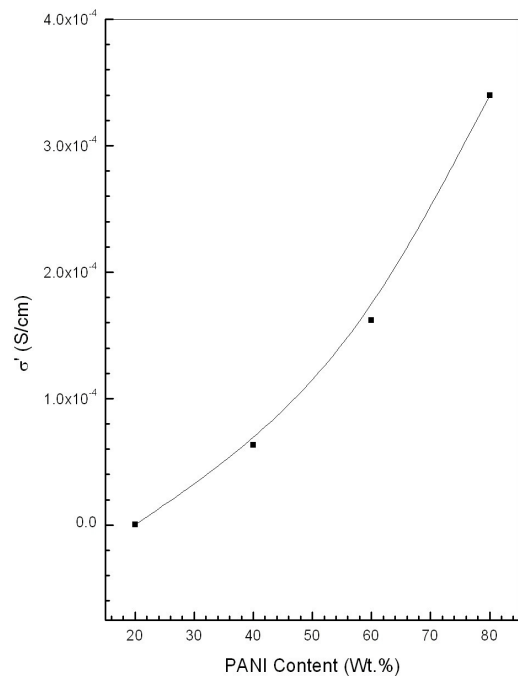


Figure 6: AC conductivity of SA/PANI composite as a function of PANI content in the composite at 10 kHz

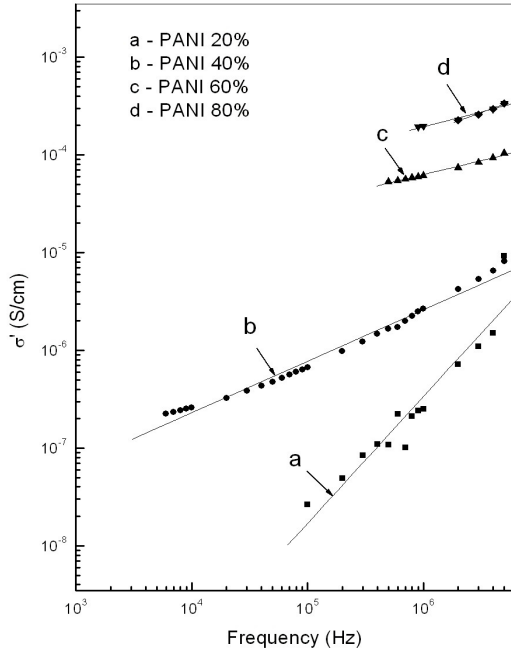


Figure 7: Log-Log plots for AC conductivity of SA/PANI composites

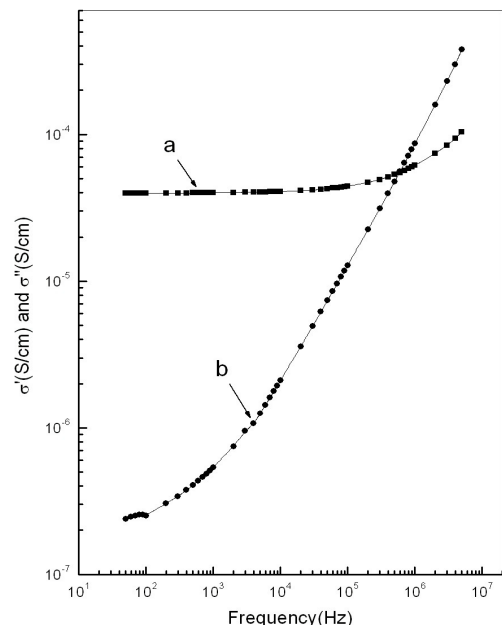


Figure 8: Plot of AC conductivity with frequency for SA/PANI-60% composite to obtain critical frequency; a) Real part and b) Imaginary part of conductivity

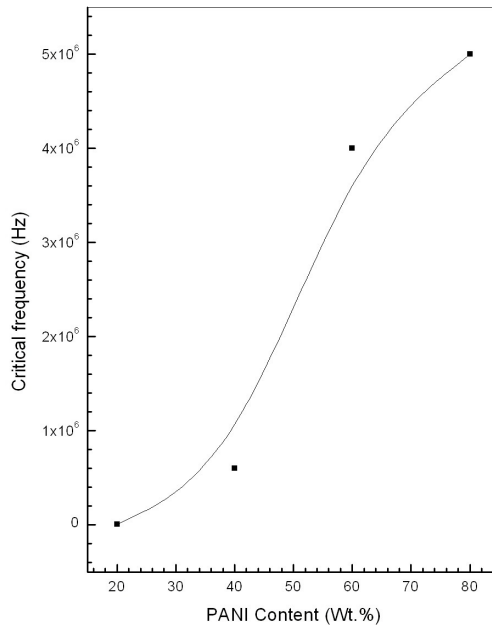


Figure 9: Critical frequency of SA/PANI composites as a function of PANI content

Table 1
Summary of AC electrical response of SA/PANI composites

S.N.	Composition, wt% PANI	Real conductivity at 10 kHz, σ' (S/cm)	Power law index, s	Critical frequency, f_c (Hz)
1	20	2.60×10^{-7}	0.60	4000
2	40	6.36×10^{-5}	0.36	600000
3	60	1.62×10^{-4}	0.30	4000000
4	80	3.98×10^{-4}	0.28	5000000

Table 2
Values of the electrical components for equivalent circuit of SA/PANI-60% composite

Index	Parameters	Values*
1	C	3.23×10^{-19}
	R	1.107×10^4
2	C	2.719×10^{-11}
	R	130.3
3	C	2.287×10^{-11}
	R	8.115×10^4
4	C	1.181×10^{-10}
	R	3.582×10^5
5	C	9.868×10^{-12}
	R	2.05×10^4

R in Ohm and C in Farad;

*Measurement errors in impedance data < 0.759%

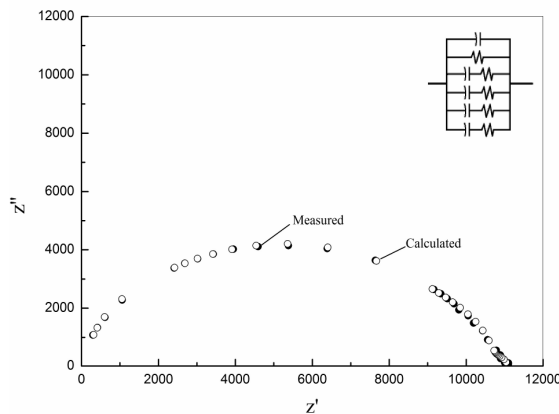


Figure 10: Complex plane impedance plot for SA/PANI-60% composite

The complex plane impedance plot for SA/PANI-60% composite was obtained by plotting the imaginary part of impedance Z'' with the real part of impedance Z' , and then simulated through the software ZsimpWin 3.21 (shown in Fig. 10). It has been observed that there is strong coherence between the measured data and calculated data in the measured frequency range of 10 Hz to 5 MHz. For SA/PANI-60% composite, semicircular shape of the plot indicates that the contribution to conductivity from grain boundaries is higher than that from the grains. Further, the relaxation nearly follows Debye's model with a single relaxation.¹³ However, the presence of a single semicircle for the composite is represented by the RC circuit of real RC elements connected in parallel (shown in the inset of Fig. 10). The corresponding RC values of the network simulated through the software are given in Table 2. According to Dyre, such an electrical circuit is a simple representation of an amorphous semiconductor, in which charge transport occurs via the electron hopping mechanism.¹⁴

Humidity sensing studies

The variation of impedance with relative humidity for SA/PANI-60% composite is shown in Fig. 11. The decrease in impedance or increase in conductivity with increasing humidity can be attributed to the mobility of SA ions, which are loosely attached to the polymer chain by weak van der Walls forces of attraction. At low humidity, the mobility of SA ions is restricted, maybe due to curling up of polymer chains under dry conditions.¹⁵ On the contrary, at high humidity, the polymer may absorb water

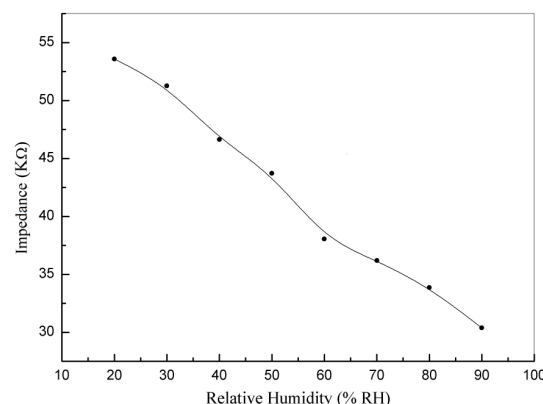


Figure 11: Variation of impedance with relative humidity for SA/PANI-60% composite

molecules followed by the uncurling of the compact coil form into straight chains that are aligned with respect to each other. This geometry of the polymer might have favoured enhanced mobility of SA ions across the polymer chains causing increased conductivity. Also, a single semicircle with five RC elements in parallel for the composite (inset of Fig. 10) obtained from the complex plane impedance plot may be due to uniform distribution of CMC particles in the PANI matrix, which might have improved the contact between each grain via its grain boundary, resulting in improved sensitivity.

CONCLUSION

In the present work, SA/PANI composites were successfully synthesized by chemical polymerization of aniline in the presence of SA. The interaction of PANI with SA and the crystallinity of the composites were confirmed by FTIR and XRD spectra. The formation of submicron particles in the composites due to SA was confirmed by SEM studies. The study has shown that the AC conductivity obeyed the power law above a critical frequency for each composite and the conductivity increased with the increase in PANI content in the composite. In particular, impedance studies on SA/PANI-60% composite shows a single semicircle on a complex plane impedance plot, indicating that the composite obeyed the Debye model with single relaxation. Based on the results, the resistive type humidity sensing ability of SA/PANI-60% composite was tested. SA/PANI composites have proved to be promising materials for devising humidity sensors.

ACKNOWLEDGEMENTS: The authors are thankful to University Grants Commission, New Delhi, for the financial support provided under major research project (41-917/2012 (SR) dated: 23/07/2012), to carry out this work.

REFERENCES

- ¹ R. F. Valentini, T. G. Vargo, J. A. Gardella and P. Aceischer, *Biomaterials*, **13**, 193 (1992).
- ² S. J. Davies, T. G. Rayan, C. J. Wilde and G. Beyer, *Synthetic Met.*, **69**, 209 (1995).
- ³ G. P. Alginates, *Carbohyd. Polym.*, **8**, 161 (1988).
- ⁴ S. Yuk, S. H. Cho and H. B. Lee, *J. Control. Release*, **7**, 69 (1995).
- ⁵ P. R. Hari, T. Chandy and C. P. Sharma, *J. Appl. Polym. Sci.*, **59**, 1795 (1996).
- ⁶ B. Smita, S. Sridar and A. A. Khan, *Eur. Polym. J.*, **41**, 1859 (2005).
- ⁷ M. V. Kulkarni and A. K. Vishwanath, *Eur. Polym. J.*, **40**, 379 (2004).
- ⁸ A. G. MacDiarmid, *Synthetic Met.*, **125**, 11 (2002).
- ⁹ M. Ghorbani, M. S. Lashkenari and H. Eisazadeh, *Synthetic Met.*, **161**, 1430 (2011).
- ¹⁰ X. Lu, W. Zhang, C. Wang, T. C. Wen and Y. Wei, *Prog. Polym. Sci.*, **36**, 671 (2011).
- ¹¹ C. Basavraja, J. K. Kim, P. X. Thinh and D. S. Huh, *J. Polym. Compos.*, **33**, 154 (2012).
- ¹² D. Hui, R. Alexandrescu and M. Chipara, *J. Optoelectron. Adv. M.*, **3**, 1700 (2001).
- ¹³ Y. T. Ravikiran, M. T. Lagare, M. Sairam, N. N. Mallikarjuna, B. Sreedhar, *et al.*, *Synthetic Met.*, **156**, 1139 (2006).
- ¹⁴ J. C. Dyre and T. B. Schroder, *Rev. Mod. Phys.*, **72**, 873 (2000).
- ¹⁵ A. T. Ramaprasad and V. Rao, *Sensor. Actuat. B*, **148**, 117 (2010).